Cronfa - Swansea University Open Access Repository

Accepted Manuscript

This is a PDF file of an unedited manuscript that has been accepted for publication. As a service to our customers we are providing this early version of the manuscript. The manuscript will undergo copyediting, typesetting, and review of the resulting proof before it is published in its final form. Please note that during the production process errors may be discovered which could affect the content, and all legal disclaimers that apply to the journal pertain.

The influence of arsenic alloying on the localised corrosion behaviour of magnesium

G. Williams [a, *], H. Ap-Llwyd Dafydd [a], H.N. McMurray [a], N. Birbilis [b]

[a] *Materials Research Centre, College of Engineering, Swansea University, Bay Campus, Crymlyn Burrows, Swansea SA1 8EN, United Kingdom*

[b] *Department of Materials Science and Engineering, Monash University, Clayton, VIC, Australia.*

* Corresponding author: geraint.williams@swansea.ac.uk, Tel: +44 (0)1792 295589

Abstract: An in-situ scanning vibrating electrode technique is used to investigate the effect of alloyed arsenic on magnesium immersed in chloride containing aqueous solution, both in freely corroding and anodically polarised conditions. Arsenic is shown to strongly suppress cathodic activation of the corroding Mg even under circumstances where breakdown has occurred and subsequent propagation of dark filiform-like tracks is observed. Under galvanostatic anodic polarisation, rates of hydrogen evolution are significantly mitigated compared to pure Mg and no time-dependent evolution of local cathodic sites is detected. The findings support the theory that cathodic activation of the dark corroded Mg surface is associated with accumulated transition metal impurity, which in turn become poisoned towards cathodic hydrogen evolution by the presence of As. In addition, these preliminary studies suggest that alloying with a strong cathodic poison may provide a means of producing a more-charge effective anode material for primary sea-water activated Mg batteries.

Keywords: Magnesium; Scanning vibrating electrode technique; Localised corrosion; Arsenic; Hydrogen evolution

1. Introduction

The poor corrosion resistance of magnesium (Mg) and its alloys currently presents a significant obstacle to its mainstream use as a lightweight structural material [1, 2]. Of the approaches used to reduce corrosion rates, one of the most attractive routes is by alloying with an element which imparts intrinsic corrosion resistance [3]. This precludes the need to rely on protection by surface treatments and coatings which form a physical barrier, isolating the underlying Mg from a potentially corrosive environment, but invariably add extra cost to any Mg-based product. A significant breakthrough in producing an intrinsically corrosion resistant form of Mg, by alloying with a low level of an Arsenic (As) addition was recently reported by Birbilis *et al* [4]. Alloy design was influenced by a previous investigation on the influence of dissolved arsenate salts in a sodium chloride test solution, which produced a profound inhibition of corrosion rates observed for commercially pure Mg [5]. In both studies it was proposed that elemental As acted as a strong cathodic poison which deactivated iron-containing impurity phases towards cathodic hydrogen evolution [4, 5].

The dependence of corrosion rate on iron (Fe) impurity level has been known since the publication of seminal works by Boyer [6] and Hanawalt [7], who proposed that iron-rich second-phase particles comprise the principal sites of cathodic hydrogen evolution. A tolerance limit of approximately 170 ppm Fe was demonstrated, above which corrosion rates increased dramatically and explained on the basis that the threshold represents a situation where iron containing second-phase particles become too large to be covered over by a protective surface film. Recent investigations have thrown more light on the role of iron impurity by demonstrating considerable cathodic activation of the previously anodically attacked Mg surface, either after undergoing corrosion at open circuit conditions [8 – 10], or following prior anodic polarisation [11, 12]. The extent of cathodic activation has also recently been shown, by means of scanning vibrating electrode (SVET) studies, to be

strongly dependent upon the iron impurity content of the Mg [13]. The origin of this cathodic activation has been the subject of much contemporary research in the field of Mg corrosion science [14 – 17]. High resolution microscopic analysis of the corroded, cathodically active regions on pure Mg has revealed evidence of sub-micron iron particles within the surface oxide layer [18], while a Rutherford Backscatter Spectroscopic (RBS) investigation demonstrated Fe impurity enrichment at the Mg-oxide interface [19] following anodic dissolution. Based on this evidence, Lysne et al [20] proposed a model of cathodic activation based on iron-rich impurity accumulation based on phases remaining electrically connected to the Mg matrix during anodic dissolution. Others have recently presented a new theory of iron impurity enrichment, based on iron rich phases becoming detached from the matrix and undergoing rapid self-corrosion followed by re-plating on the newly corroded Mg surface [21]. It would therefore seem plausible therefore, that the presence of a strong cathodic poison, such as As [22] as an alloying addition, should act to limit hydrogen evolution on accumulated iron-rich impurity deposits.

The principal aim of the investigation reported herein is to expand on the preliminary work, recently published in a previous short communication on the origin of the corrosion resistance of As-alloyed Mg [4]. In this work an in-situ SVET is employed to visualise time-dependent localised corrosion pattern changes for both freely corroding Mg-As and pure Mg to fully describe the mode(s) by which alloyed As acts to significantly retard the rate of corrosion. Conditions are employed which produce breakdown in the Mg-As alloy, along with subsequent evolution of a dark, film covered surface, which in the absence of As has previously been demonstrated to act as a site of enhanced cathodic activity when compared with the original uncorroded Mg [8, 9]. A second aim is therefore to ascertain whether the presence of As significantly influences cathodic current density values on the cathodically activated, corroded Mg surface. In addition, we have also sought to use SVET analysis to

compare and contrast localised corrosion patterns obtained under galvanostatic anodic polarisation for both Mg and Mg-As. Previous studies using pure Mg have demonstrated that progressively higher rates of hydrogen evolution are observed as the specimen potential is increased above its free corrosion potential. A further aim of this work is to determine whether or not alloyed As influences hydrogen evolution rates under imposed anodic polarisation and to identify whether the Mg-As alloy demonstrates promise as a self-discharge resistant primary battery anode.

2. Experimental

2.1 Materials

All experiments were carried out using 99.99% high purity Mg, with the principal impurity elements being Fe (40 ppm), Ni (10 pm) and Cu (20 ppm). An Mg-As alloy was produced by initially encapsulating quantities of the Mg and As (sourced from Alfa-Aeser, USA) in a quartz tube. This was backfilled with high purity argon to avoid any reaction of the Mg with the atmosphere and to contain any molten As. To avoid reaction of any molten metal with the quartz itself, the inside of the tube was coated with graphite prior to encapsulation. The charge was held in the molten state at 700°C for 3 minutes, and periodically agitated to ensure mixing. The alloy was then left to cool in air, removed from encapsulation by breaking the quartz, and tested in this condition. The chemical composition of both pure Mg and the Mg-As alloy were independently analysed using ICP-OES (Spectrometer Services, Coburg, Victoria, Australia). The alloy preparation route described above resulted in the successful formation of an Mg-0.37 wt.% As alloy. The alloy microstructure has been reported elsewhere [4], showing that the majority of the alloyed As is present as an Mg_3As_2

precipitate within an α-Mg matrix, with only a small amount (< 0.01%) existing in solid solution.

2.2 Methods

SVET investigation of Mg and Mg-As alloy specimens was carried out in both unpolarised (i.e. freely corroding) conditions and under anodic polarisation. The SVET instrument employed a probe consisting of a platinum wire (125 µm, Goodfellow metals Ltd) sealed in a glass sheath so that vibrating electrode comprised a 125 µm diameter Pt micro-disc electrode. Full details of SVET instrument design and calibration procedure are given in previous publications [8, 23]. After making electrical connection to Mg and Mg-As alloys specimens, they were cold mounted in two-part epoxy resin so that a minimum area of ca 30 mm^2 was showing. The exposed surfaces were abraded using silicon carbide paper and polished using an aqueous slurry of 5 µm polishing alumina, washed with aqueous surfactant and rinsed with distilled water followed by ethanol. Sample surfaces were completely immersed in an electrolyte bath containing aqueous sodium chloride electrolyte at concentrations in the range 0.1 – 2 mol dm^{-3} at pH 6.5 and a temperature of 20°C. The SVET probe was held vertically and scanned at a constant of height of 100 µm above the exposed surface. For anodically polarised specimens, current densities values in the range 0.4 to 1.0 mA cm^{-2} were applied by means of micro-galvanostat of in-house construction, employing a Pt gauze counter electrode. SVET scans were carried out immediately following the start of polarisation and at 4 min intervals thereafter for periods of up to 3h. The matrix of SVET-derived peak-to-peak voltage values comprising each scan was converted to values of current flux density along the axis of probe vibration (j_z), by applying a calibration factor determined by galvanostatically checking the calibration using a two-compartment cell containing the relevant NaCl (aq) electrolyte, as described previously [8]. In the concentrated electrolytes of 0.1 mol dm^{-3} NaCl

(aq) and above used here, the assumption is made that any local conductivity increases at anode and cathode sites will be negligible in comparison with the high bulk electrolyte conductivity. In addition, the fact that the probe tip is scanned at a height of 100 μm above the corroding surface also mitigates the likelihood of interference of surface accumulation of ionic species on the accuracy of the SVET measurement.

Bulk hydrogen evolution rates were determined using volumetric measurements, employing an arrangement consisting of an upturned, electrolyte filled burette and glass funnel [24]. Potentiodynamic experiments in electrolytes containing varying sodium chloride concentration were carried out using a Solartron 1280B workstation in conjunction with a conventional 3 cell arrangement. This consisted of a Pt gauze counter electrode and saturated calomel (SCE) reference electrode using a Luggin capillary to minimize any ohmic drops possible when using dilute chloride concentrations.

3. Results and Discussion

3.1 Characterisation of localised corrosion under freely corroding conditions

Previously published results, using a combination of mass loss and volumetric hydrogen capture to compare the bulk corrosion rates of pure Mg in the presence and absence of alloyed As, showed that significantly higher corrosion resistance was observed for the latter upon immersion in 0.1 mol dm^{-3} NaCl (aq) [4]. Furthermore, potentiodynamic experiments carried out in the same electrolyte suggested that a marked retardation of cathode kinetics was primarily responsible for the significantly lower corrosion rate determined for the Mg-As alloy. To further elucidate the role of As, we have employed in-situ SVET to compare and contrast the same Mg-As alloy with pure Mg, in terms of time-dependent changes in current density distributions observed over their surfaces when immersed under freely corroding

conditions in 0.1 mol dm^{-3} NaCl (aq). The localised corrosion behaviour of pure Mg (40 ppm Fe impurity) is discussed at length elsewhere [8] and will only be briefly re-capped here.

Figure 1 shows SVET-derived surface maps of current density measured along the axis of probe vibration (j_z) obtained (a) 4 and (b) 20 h following immersion in 0.1 mol dm^{-3} NaCl (aq) at pH 7. During the initial stages of immersion, the pure Mg surface is shown to be largely electrochemically inactive. However, after an induction period of ca 1h, breakdown of the temporarily passive Mg surface was observed, leading to the appearance of one or more dark spots on the surface from which rising streams of fine hydrogen bubbles was observed to emanate. These dark spots developed into tracks which lengthened with time and which SVET scanning revealed as comprising of a highly focal anode at the leading edge, coupled with a cathodically activated region behind which correlated with the location of the previously corroded (dark) surface. The behaviour is typified in Figure 1 (a), which shows the distribution of current density values associated with a population of propagating dark tracks which initiated close to the left hand edge of the exposed area and have moved up to 1 mm from their original point of initiation. The situation at a longer immersion time is demonstrated in Figure 1 (b), which shows that the previously anodically surface remains a net local cathode many hours after originally being revealed following forward movement of the principal sites of local Mg dissolution. The photographic image of the corroded surface after removal from the corrosive electrolyte after 24h immersion, given in Figure 1 (c) shows how the dark corroded regions correspond with the electrochemically active regions in 1 (b).

Under identical conditions and over the same timescale, the localised corrosion behaviour of the Mg-As (0.37%) alloy differed considerably, as demonstrated in Figure 2, where SVET-derived j_z distribution maps corresponding to similar immersion times as previously are given. Both surface maps recorded at 4h and 20h (see Figures 2(a) and (b), respectively) show that the majority of the exposed surface acted as a distributed anode where

typical anodic current density values were in the +1 to +5 A m^{-2} range. This low-level, large area anode was coupled with several focal cathode sites, located towards the right hand side of the maps given in Figures 2(a) and (b). Very little change in the j_z distributions was observed over 24h, although j_z values in the anodic region gradually decreased with time to fall within the 0 to +2 A m^{-2} range when the experiment was terminated. The behaviour is consistent with previous results obtained for commercially pure (CP) Mg prior to breakdown [8], although it should be borne in mind that the situation in this particular case only persists for several minutes following immersion. The post-corrosion surface (see Figure 2c), shows no evidence of any dark film covered regions and the entirety of the surface remains bright, albeit showing evidence of being roughened/etched on a microscopic length-scale. The region which was shown to correspond to a persistent local cathode in the lower right corner of the corroded surface appears to be covered in several dome-like solid deposits. On the basis that sustained cathodic hydrogen evolution occurs at this location, in turn producing increased local alkalinity, it seems plausible to propose that these deposits comprise magnesium hydroxide, formed as local concentrations of hydroxide and magnesium cations exceed the solubility product threshold for $Mg(OH)_2$ ($K_s = [Mg^{2+}][OH^-]^2 = 3.0 \times 10^{-11}$ mol^3 dm^{-9} [25]).

It seems therefore that the low rates of corrosion for Mg-As reported previously [4] in 0.1 mol dm^{-3} NaCl (aq) derive principally from the ability to withstand breakdown and subsequent conversion of the uncorroded Mg to a dark, cathodically-activated film-covered surface. Previous investigations have demonstrated that time-dependent corrosion rates observed post-breakdown rise in proportion to the total area occupied by the cathodically enhanced dark film [8], and that for the initial stages of Mg corrosion, the overall process is under cathodic control. A relatively constant E_{corr} value of -1.70 V vs SCE was determined for the Mg-As alloy immersed in 0.1 mol dm^{-3} NaCl (aq) over a period of 4h. This is evidently more negative than the -1.62 V vs SCE established for pure Mg under the same

conditions. It therefore seems plausible that the obvious suppression of cathodic activity by alloyed As produces a depression in E_{corr} such that the potential remains well below that required for spontaneous breakdown of the Mg-As alloy to occur (i.e the apparent breakdown potential, E_b).

To test out this hypothesis, the concentration of the NaCl (aq) was increased significantly and the same immersion experiments were carried out in conjunction with in-situ SVET analysis. The aim was to gauge whether or not the markedly increased chloride concentration would induce breakdown in the Mg-As. In addition, should breakdown occur, producing a dark corroded surface, a second aim was to determine if the presence of As influenced the degree of cathodic activation observed for such a feature. Previous work has shown that for commercially pure Mg [26] and AZ31 alloy [27], which undergo spontaneous breakdown in the absence of external polarization when immersed in chloride electrolyte, an apparent breakdown potential E_b could be established by following inflections in time-dependent behaviour of free corrosion potential (E_{corr}). E_b was shown to become progressively more negative with increasing [Cl⁻] and for pure Mg, a dependence of E_b on [Cl⁻] was established such that $E_b = A + B \log_{10}[Cl^-]$, where the value of B was -0.11 V per decade. It was also demonstrated that at a point where $E_{corr} \geq E_b$, breakdown occurred, marked by the first appearance of a dark, corroded region which evolved hydrogen strongly. In situations where spontaneous breakdown did not occur under unpolarised conditions, the same E_b vs [Cl⁻] relationship could be determined from polarisation curves obtained at different chloride ion concentrations in potentiodynamic experiments. For the Mg-As alloy studied in this work, which does not spontaneously undergo breakdown, this latter approach was used to confirm the same dependence of E_b on [Cl⁻].

Typical polarization curves observed for Mg-As(0.37%) in aqueous electrolytes containing varying sodium chloride concentrations over several orders of magnitude are

given in Figure 3. A clear inflection in the anodic branches of curves ii – vi is seen, signifying apparent passive breakdown and trans-passive behaviour shown as a rapid increase in anodic current density with applied potential. This indication of passivity breakdown in the anodic braches of the polarization curves also becomes progressively well-developed as $[Cl^-]$ is decreased. The potential at which the inflection was observed was used as the value of breakdown potential E_b. Average values of breakdown potential (E_b), taken at the point of sharp inflection in anodic polarization curves for multiple repeat experiments, showed a clear dependence on $[Cl^-]$ (see Figure 4), confirming the relationship, $E_b = A + B \log_{10} [Cl^-]$, where A = -1.68 V vs SCE and B = -0.104 V/decade for this particular alloy. The horizontal dashed line in Figure 4 indicates the time-independent value of E_{corr} measured in a separate experiment for Mg-As immersed in 2 mol dm^{-3} NaCl (aq), showing that it intersects with the E_b vs $\log_{10} [Cl^-]$ plot at point close to this particular concentration. For lower chloride ion concentrations, E_b was always markedly more positive than values of E_{corr} established in the absence of external polarization.

Under immersion in freely corroding conditions in 2 mol dm^{-3} NaCl (aq), the predicted occurrence of breakdown was indeed observed, although there was a ca. 15h delay until repetitive SVET-scanning revealed the first point of breakdown. A sequence of SVET-derived j_z distribution maps obtained post-breakdown, capturing the propagation of a dark corrosion track traversing from left to right over the exposed Mg-As surface is given in Figure 5. The location of the single focal anode, observed in Figures 5 a – c coincides with the leading edge of the lengthening track of dark filmed surface. An image of the corroded surface given in Figure 2 (d), taken after 24h immersion, confirms that a significant proportion of the Mg-As surface had corroded to produce a dark film. However, as the anode advanced, there was no evidence of cathodic current emerging from the dark corroded surface left behind. This again contrasted with the behaviour of pure Mg under the same conditions,

where repetitive SVET scanning of the corroding surface in 2 mol dm^{-3} NaCl (aq) again confirmed cathodic activation of the corroded regions. A series of typical j_z distribution maps, recorded after the breakdown of a pure Mg surface, showing a cathodically enhanced region develop immediately behind a local anode at the front of an advancing corrosion track, is shown for comparison in Figures 6 (a -c), along with a photographic image of the corroded surface taken after 24h (see Figure 6 d).

The difference in behaviour is perhaps more apparent in Figure 7, which shows profiles of j_z versus distance, taken at different times along propagating corrosion filaments on either pure Mg or Mg-As (0.37%) indicated by the arrows in Figs 5c and 6c. These plots again confirm that the leading edge of each the filament is a focal anode, with a peak j_z value of ca. +180 A m^{-2} for pure Mg (Fig 7a) which appears to remain constant with time as the advance of the filament proceeds. The corroded "track" left behind the advancing filament is shown to become cathodically activated with respect to the uncorroded surface, giving measured j_z values of up to -15 A m^{-2} in regions extending several mm behind the local anode. The profiles are similar in nature to those previously reported for commercially pure Mg corroding in 5% w/v NaCl (aq) [8], where the main corrosion features observed are dark expanding discs rather than filiform-like corrosion, although the cathodic j_z values measured for corrosion features on high purity Mg studied here are over an order of magnitude lower. Peak j_z values observed for Mg-As (0.37%) were generally significantly lower at ca. +100 A m^{-2} and all j_z values measured over the corroded surface (i.e. to the left of the j_z peak) were $\geq$ 0 A m^{-2} and no different to the original intact (uncorroded) Mg-As surface.

It is therefore apparent that the presence of As strongly suppresses cathodic activity on the previously anodically attacked Mg. This finding is highly noteworthy, since the origin of cathodic activation of Mg on a previously corroded surface is currently the focus of considerable attention. The current consensus is that enhanced electrocatalytic activation

towards hydrogen evolution arises because of the accumulation of transition metal impurities, principally iron, on the Mg surface during anodic dissolution [14]. Hoche et al recently proposed that the impurity enrichment arises through a mechanism involving detachment of transition metal-rich phases from the Mg matrix and subsequent re-plating following rapid self-corrosion of these detached particles [21]. In addition, others have emphasised the importance of the nature of the oxide covered surface [28], which in the case of the cathodically active dark film, has been found to differ considerably in nature when compared to the surface of the uncorroded Mg [18]. The observation of As acting to stifle cathodic activity on the dark film would therefore tend to support the fact that the principal cathode sites indeed derive from accumulated iron impurity deposits. It is known that strong cathodic poisons such as As [29, 30] have a considerable influence on the kinetics of hydrogen evolution on various metal surfaces, including transition metals such as Fe, by decreasing surface coverage by the adsorbed H atom intermediate and therefore the rate of H atom recombination. In previous work it was proposed that reduced hydrogen evolution rates on corroding Mg were principally due to the presence of elemental As ad-atoms on the local noble metal impurity cathode sites which act to block H atom recombination [4]. The observations made herein seem to validate this hypothesis by demonstrating that local current density values measured on local cathode sites decrease from ca -15 A m^{-2} to zero in the presence of a low level As alloying.

Finally, a question arises as to whether or not the observed breakdown of the Mg-As alloy in 2 mol dm^{-3} NaCl (aq) electrolyte influences the bulk rate of corrosion when compared with pure Mg. Previously, we had proposed that the low corrosion rates observed in more dilute NaCl (aq) concentrations stemmed to the ability of the As additions to impart resistance to breakdown by keeping the free corrosion potential well below the apparent breakdown potential. Average corrosion rates of 0.044 and 0.002 cm^3 H$_2$ per cm^2 area over a

one week immersion period, determined by a volumetric method, were measured previously for Mg and Mg-As (0.37%) respectively [4]. Similar studies carried out as part of this present investigation for specimens immersed in 2 mol dm^{-3} NaCl over 7 days, determined an average quantity of 0.050 ± 0.02 cm^3 evolved H_2 per cm^2 area for pure Mg, which is only marginally higher than that established in the more dilute electrolyte. For Mg-As (0.37%), where breakdown and subsequent evolution of a dark surface film was observed, a corrosion rate of 0.008 ± 0.005 cm^3 H_2 per cm^2 area wk^{-1} was measured, which despite being significantly greater than that observed in 0.1 mol dm^{-3} electrolyte, remains markedly lower (by a factor of > 5) than pure Mg. It seems therefore that the suppression of any cathodic activation of the dark film covered Mg surface by As additions is principally responsible for the decreased rate of corrosion observed on a post-breakdown Mg surface.

3.2 Localised corrosion behaviour under anodic polarisation

It has been shown elsewhere [12] that when pure Mg is polarised to potentials which are more positive that its open circuit potential (OCP), then the evolution of a dark, cathodically film-covered surface occurs more rapidly than under freely corroding conditions. Furthermore, at imposed galvanostatic current density values in the range +0.4 to +2 mA cm^{-2}, the rate of area conversion of intact (uncorroded) surface to local cathode sites increased progressively with applied current density. Numerical integration of SVET-derived local current distributions showed that time-dependent anodic current emerging from the polarised electrode increased in proportion to the total cathodic current measured over growing local cathode areas, and that trends observed at different imposed anodic current density values matched those observed using bulk hydrogen collection measurements. The results confirmed that "parasitic" hydrogen evolution at a dissolving Mg anode originates from a localised cathodic reaction which consequently produces a significantly higher Mg loss than theory

would predict from the net charge passed within the external circuit connecting the working and counter electrodes.

In light of the ability of alloyed As to suppress cathodic activation of the post-breakdown, dark, corroded Mg surface at OCP, its efficiency in mitigating parasitic hydrogen evolution at imposed potential > E_{corr} was also briefly investigated. In-situ SVET results obtained for both Mg and Mg-As (0.37%) under an applied anodic current density of 0.4 mA cm^{-2} when immersed in 0.1 mol dm^{-3} NaCl (aq) are typified by the surface maps of j_z distributions given in Figure 8. For pure Mg at galvanostatic holding periods of 1h and 2h, shown in Figures 8a and 8b respectively, the behaviour closely follows previously published results obtained in a more concentrated NaCl (aq) electrolyte. The leading edges of the dark tracks which develop on the working electrode immediately after applying the +0.4 mA cm^{-2} galvanostatic current are shown to be intense local anodes. As these advance over the exposed surface, the regions left behind become local cathode sites which occupy progressively more of the total exposed area with time. However, under the same conditions and timescale the Mg-As alloy behaves entirely differently. Figures 8c and 8d show j_z distribution maps obtained for Mg-As at 1h and 2h holding periods respectively, using the same scaling as the results shown for pure Mg. In this case, the electrode surface is shown to be a large area distributed anode where j_z values lie in the range +2 to +6 A m^{-2}. There was little change in behaviour even at protracted polarisation times up to 4h and no evidence of onset of local cathode sites could be detected. Visual examination of the post-corrosion surface showed no evidence of the presence of a dark film. It seems plausible therefore to propose that the homogeneous dissolution pattern of the Mg-As anode results from the ability of the Mg-As to withstand breakdown, even under an imposed anodic current.

In a separate experiment, the imposed anodic current density was increased to +1 mA cm^{-2} to observe whether or not breakdown could be induced and to subsequently investigate

post-breakdown localised corrosion characteristics. Under these conditions, the patterns of local anodic activity change considerably and several focal anode sites showing peak j_z values of up to 60 A m^{-2} develop within 30 min of applying the galvanostatic current. With time, these sites become more numerous and local anode patterns are typified by the j_z surface map given in Figure 9a, which was obtained after 2h polarisation. However, even in a post-breakdown condition, where highly focal anode sites exist on the polarised Mg-As surface, no local cathode sites could be visualised, even at holding times of up to 6h. Visual examination of the Mg-As surface following polarisation showed some evidence of dark corroded regions (see Figure 9c), but in comparison with pure Mg maintained under the same conditions (Figure 9b), the surface coverage was far less extensive and in general the corroded tracks were much narrower and limited in terms of length.

Time-resolved SVET data, typified by the results given in Figure 8 can be effectively condensed by numerical area integration of j_z distributions [8, 12, 31, 32], to give values of total anodic current (I_a) and cathodic current (I_c) for each scan. Figure 10 shows how values of I_a and I_c obtained for both Mg and Mg-As vary with time during galvanostatic polarisation at +0.4 mA cm^{-2} in a 0.1 mol dm^{-3} NaCl (aq) electrolyte. In the early stages of the experiment, I_a measured over a 1 cm^2 pure Mg area closely agrees with the applied current (I_{appl}), shown by the horizontal dashed line in Fig 10. However, when local cathode sites become established and grow with time, then a progressive increase in I_a is observed (Fig 10, red plot). This coincides closely with a similar time-dependent increase in I_c (Fig 10, blue plot). In contrast, the results obtained for Mg-As show little or no time-dependent change in I_a along with zero values of I_c at all times.

Hydrogen collection experiments were carried out using the same conditions to investigate whether this obvious modification of Mg anode behaviour by As alloying translated to strongly mitigated hydrogen evolution rates under anodic polarisation. The

results given in Figure 11 demonstrate the divergence in behaviour of Mg-As compared with pure Mg at two different applied current density values of +0.4 A m^{-2} (see green plots) and +1 A m^{-2} (black plots). The rates of hydrogen evolution at both values of I_{appl} are markedly lower in the case of the Mg-As alloy; for example, a rate of 2.3×10^{-4} mol H$_2$ m^{-2} min^{-1} established for Mg after 2h polarisation using of I_{appl} = +0.4 mA cm^{-2}, decreased by an order of magnitude to 2×10^{-5} mol H$_2$ m^{-2} min^{-1} in the presence of alloyed As. The observation of a strongly mitigated hydrogen evolution rate observed at of I_{appl} = +1 mA cm^{-2} is also highly significant since under these conditions, breakdown of the Mg-As occurs, producing regions which comprise a dark film, which normally (for pure Mg) would constitute the onset of cathodic activation and accelerate the Mg dissolution rate. Again it would seem that As can act as a sufficiently efficient cathodic poison to deactivate the dark film produced by prior anodic attack and thus strongly decrease rates of parasitic hydrogen evolution on the dissolving Mg surface. These preliminary findings should prove meaningful to researchers seeking to utilise Mg as an anode material for primary batteries [33, 34], as a major drawback is acknowledged to be self-discharge linked to parasitic hydrogen evolution, which is manifested in a considerably lower discharge capacity than theory would predict [35, 36]. It would seem that the approach of alloying with a strong cathodic poison holds significant promise as a means of stifling "anodic" hydrogen evolution and providing a more charge effective and durable Mg–based primary anode.

4. Conclusions

In-situ SVET experiments were carried out on both high purity Mg and a novel Mg-As (0.37%) alloy to determine the influence of the addition of a strong cathodic poison on the localised corrosion behaviour of Mg both under freely corroding conditions and at applied potentials > OCP. From the results presented the following can be concluded:

- When immersed under unpolarised conditions in relatively dilute NaCl (aq) electrolytes of ≤ 0.1 mol dm^{-3}, the addition of As prevents breakdown of the Mg along with the subsequent evolution of a cathodically activated dark, film covered surface. This is achieved by suppressing cathode kinetics so that the free corrosion potential of the alloy is always more negative than its apparent breakdown potential.

- Breakdown of the Mg-As alloy is observed in a more concentrated 2 mol dm^{-3} solution, leading to the propagation of dark corrosion tracks. However, in contrast to the behaviour of pure Mg under the same conditions, no evidence of local cathodic activity in these regions is detected. The action of As in suppressing cathodic hydrogen evolution on the dark, film covered surface supports the theory that the cathodic activation normally observed for Mg derives from iron impurity accumulation.

- Under anodic polarisation at potentials > OCP no evidence of local cathodic activity could be detected on the dissolving Mg-As surface at imposed current density values of up to +1 mA cm^{-2}. Volumetric hydrogen collection measurements confirmed that rates of hydrogen evolution were reduced by up to an order of magnitude compared with pure Mg under the same conditions.

References

1. I.J. Polmear, Light alloys: metallurgy of the light metals. 3rd edn, Arnold publ., London, (1995).

2. G.L. Makar, J. Kruger, Corrosion of magnesium. International Materials Reviews 38 (1993) 138.

3. R. L. Liu, M. F. Hurley, A. Kvryan, G. Williams, J. R. Scully, N. Birbilis, Controlling the corrosion and cathodic activation of magnesium via microalloying additions of Ge, Nature Scientific Reports, 6: 28747.

4. N. Birbilis , G. Williams, K. Gusieva, A. Samaniego, M.A. Gibson and H.N. McMurray, Poisoning the corrosion of magnesium, Electrochemistry Communications , 34 (2013), 295.

5. D. Eaves, G. Williams and H.N. McMurray, Inhibition of Self-corrosion in Magnesium by Poisoning Hydrogen Recombination on Iron Impurities, Electrochim. Acta, 79, (2012), 1.

6. J.A. Boyer, The corrosion of magnesium and of the magnesium aluminum alloys containing manganese, Report-248, American Magnesium Corporation, Niagara Falls, NY, USA, 1927.

7 R.E. McNulty, J.D. Hanawalt,. Some Corrosion Characteristics of High Purity Magnesium Alloys. Transactions of the Electrochemical Society 81 (1942) 423.

8. G. Williams, H.N. McMurray, Localised Corrosion of Magnesium in Chloride Containing Electrolyte Studied by a Scanning Vibrating Electrode Technique, J. Electrochem. Soc., 155 (7), (2008) C340.

9. K.D. Ralston, G. Williams, N. Birbilis, Effect of Grain Size and ECAP on the Corrosion of High Purity Magnesium, Corrosion, 68 (2012) 507.

10. M. Curioni, The behaviour of magnesium during free corrosion and potentiodynamic polarization investigated by real-time hydrogen measurement and optical imaging, Electrochim. Acta, 120 (2014) 284.

11. N. Birbilis, A.D. King, S. Thomas, G.S. Frankel, J.R. Scully, Evidence for enhanced catalytic activity of magnesium arising from anodic dissolution, Electrochim. Acta 132 (2014) 277.

12. G. Williams, N. Birbilis and H.N. McMurray, The source of hydrogen evolved from a magnesium anode, Electrochemistry Communications, 36 (2013), 1.

13. G. Williams, N. Birbilis, and H.N. McMurray, Controlling factors in localised corrosion morphologies observed for magnesium immersed in chloride containing electrolyte, Faraday Discussions, 180, (2015) 313.

14. S. Thomas, N.V. Medhekar, G.S. Frankel, N. Birbilis, Corrosion mechanism and hydrogen evolution on Mg, Curr. Opin. Solid State Mat. Sci. 19 (2015) 85.

15. S. Fajardo, G.S. Frankel, Effect of impurities on the enhanced catalytic activity for hydrogen evolution in high purity magnesium, Electrochim. Acta 165 (2015) 255.

16. S. Thomas, O. Gharbi, S.H. Salleh, P. Volovitch, K. Ogle, N. Birbilis, On the effect of Fe concentration on Mg dissolution and activation studied using atomic emission spectr-electrochemistry and scanning electrochemical microscopy, Electrochim. Acta 210 (2016) 271.

17. S. Fajardo, C.F. Glover, G. Williams, G.S. Frankel, The Source of Anodic Hydrogen Evolution on Ultra High Purity Magnesium, Electrochim. Acta, 212 (2016) 510.

18. M. Taheri, J.R. Kish, N. Birbilis, M. Danaie, E.A. McNally, J.R. McDermid, Towards a Physical Description for the Origin of Enhanced Catalytic Activity of Corroding Magnesium Surfaces, Electrochim. Acta 116 (2014) 396.

19. T. Cain, S.B. Madden, N. Birbilis, J.R. Scully, Evidence of the Enrichment of Transition Metal Elements on Corroding Magnesium Surfaces Using Rutherford Backscattering Spectrometry, J. Electrochem. Soc. 162 (2015) C228

20. D. Lysne, S. Thomas, M.F. Hurley, N. Birbilis, On the Fe Enrichment during Anodic Polarization of Mg and Its Impact on Hydrogen Evolution, J. Electrochem. Soc. 162 (2015) C396.

21. D. Hoche, C. Blawert, S.V. Lamaka, N. Scharnagl, C. Mendis, M.L. Zheludkevich, The effect of iron re-deposition on the corrosion of impurity-containing magnesium, Phys. Chem. Chem. Phys. 18 (2016) 1279.

22. B.E. Conway, B.V. Tilak, Behavior and Characterization of Kinetically Involved Chemisorbed Intermediates in Electrocatalysis of Gas Evolution Reactions Advances in Catalysis. 38 (1992) 1.

23. G. Williams, H.N. McMurray, Pitting corrosion of steam turbine blading steels: the influence of chromium content, temperature and chloride ion concentration, Corrosion, 62 (2006), 231.

24. G. Song, Recent Progress in Corrosion and Protection of Magnesium Alloys, Adv. Eng. Mater., 7 (2005) 563.

25. Alkaline earth hydroxides in water, aqueous solutions, in: I. Lambert, H.L. Clever (Eds.), IUPAC Solubility Data Series, vol. 52, Pergamon Press, Oxford, UK, 1992, p. 104.

26. G. Williams, H. Dafydd and R. Subramanian, Chloride Ion Concentration Effects on Passivity Breakdown in Magnesium, ECS Transactions, 58(31), (2014), 23.

27. G. Williams, H. Dafydd and R. Grace, Localised corrosion of Mg alloy AZ31 in chloride-containing electrolyte studied by a scanning vibrating electrode technique, Electrochim. Acta, 109 (2013) 489.

28. S.H. Salleh, S. Thomas, J.A. Yuwono, K. Venkatesan, N. Birbilis, Enhanced hydrogen evolution on Mg (OH)$_2$ covered Mg surfaces, Electrochim. Acta 161 (2015) 144.

29. J.O'.M. Bockris, B.E. Conway, Studies in hydrogen overpotential, Transactions of the Faraday Society 45 (1949) 989.

30. P. Stonehart, G. Kohlmayr, Effect of poisons on kinetic parameters for platinum electrocatalyst sites, Electrochimica Acta 17 (1972) 369.

31. G. Williams, A.J. Coleman and H.N. McMurray, Inhibition of Aluminium Alloy AA2024-T3 pitting corrosion by copper complexing compounds, Electrochim. Acta, 55, (2010), 5947.

32. G. Williams, H.N. McMurray, R. Grace, Inhibition of magnesium localised corrosion in chloride containing electrolyte, Electrochim. Acta, 55, (2010), 7824

33. W. Li, C. Li, C. Zhou, H. Ma, J. Chen, Metallic Magnesium Nano/Mesoscale Structures: Their Shape-Controlled Preparation and Mg/Air Battery Applications, Angew. Chem. Int. Ed. 45 (2006), 6009.

34. K. Vuorilehto, An environmentally friendly water-activated manganese dioxide battery, J. Applied Electrochem. 33 (2003), 15.

35. R. Balasubramanian, A. Veluchamy, N. Venkatakrishnan, Gasometric corrosion-rate studies of magnesium alloy in magnesium batteries J. Power Sources, 52 (1994) 305.

36. Y. Ma, N. Li, D. Li, M. Zhang, X. Huang, Performance of Mg–14Li–1Al–0.1Ce as anode for Mg-air battery, J. Power Sources 196 (2011) 2346.

Figure Legends

Figure 1: Surface maps showing the distribution of current density (j_z) normal to the plane of scan above a pure Mg sample, freely corroding in aerated 0.1 mol dm^{-3} NaCl (aq) electrolyte at 20°C and pH 6.5. Data was obtained from SVET scans carried out (a) 4 h and (b) 20 h min immersion. (c) shows sample appearance after 24h immersion.
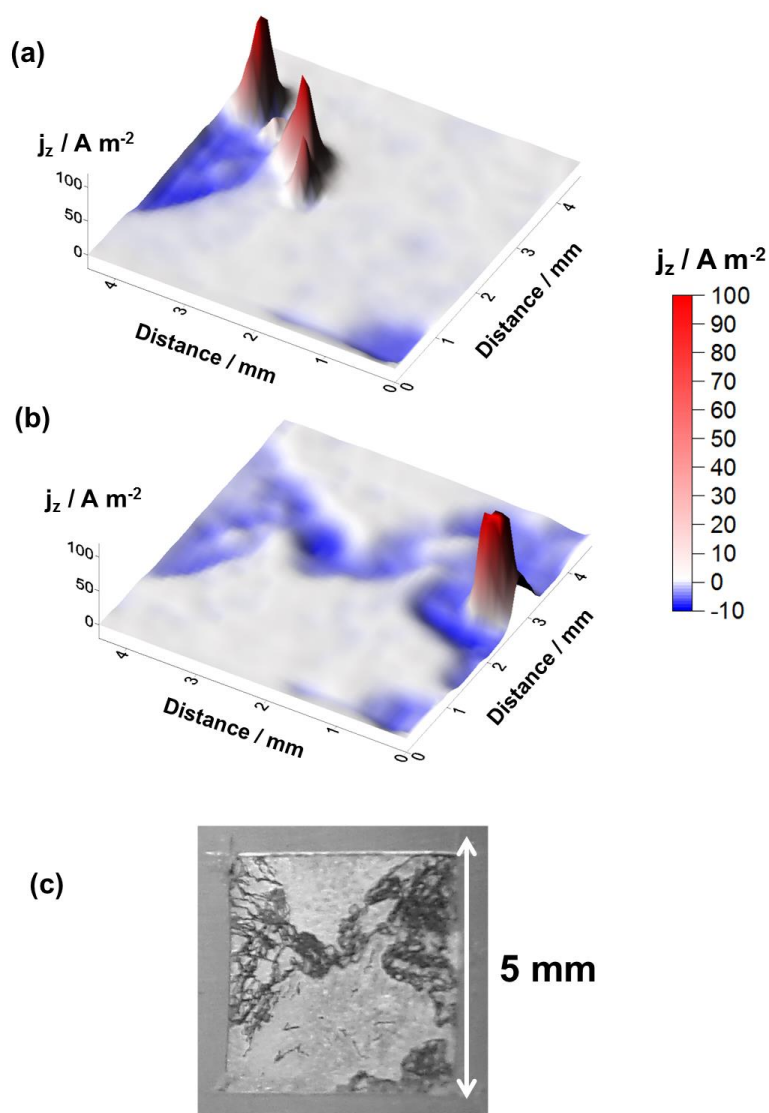
Figure 2: j_z distribution maps obtained for an unpolarised Mg-As (0.37%) alloy sample in aerated 0.1 mol dm^{-3} NaCl (aq) electrolyte at 20°C and pH 6.5 at (a) 4 h and (b) 20 h min following immersion. (c) shows sample appearance after 24h immersion.
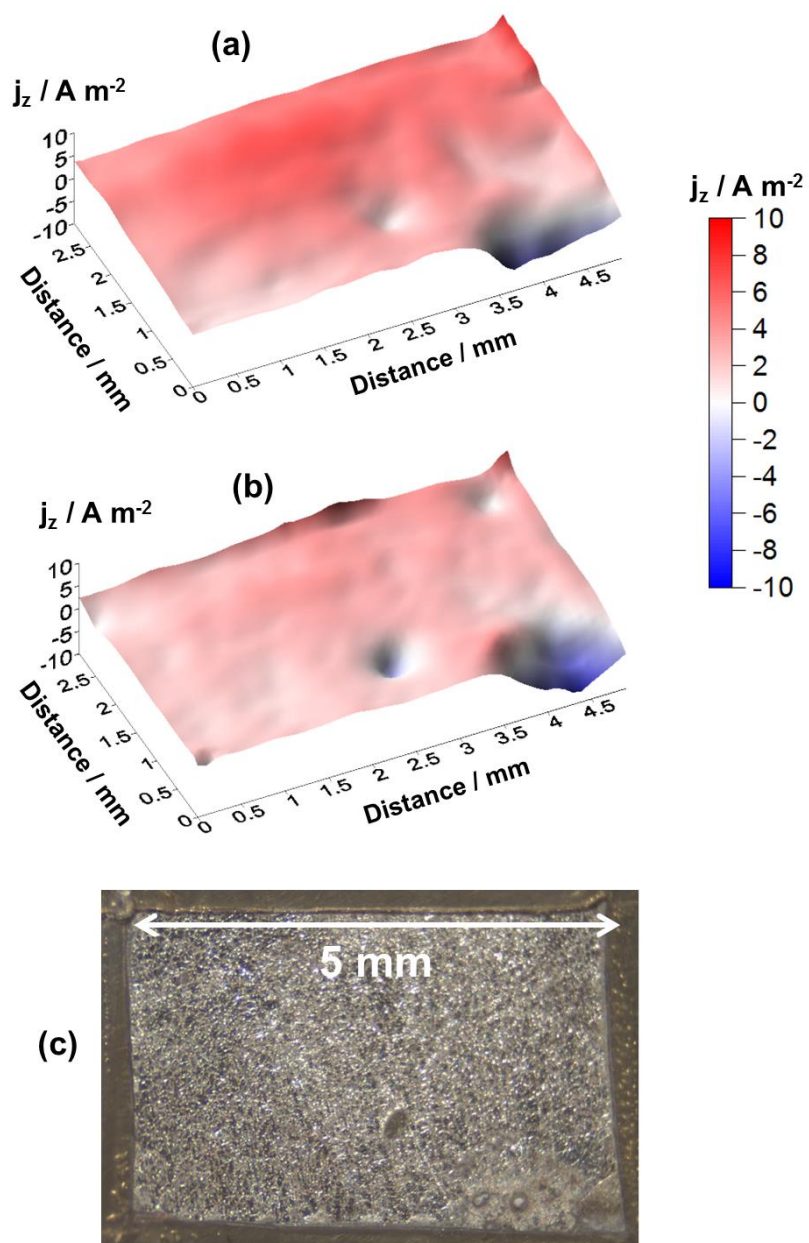
Figure 3: Anodic-going potentiodynamic polarisation curves obtained for Mg-As (0.37%) in electrolytes consisting of, i. 2, ii. 0.5, iii. 0.1, iv. 0.02 and v. 0.005 mol dm^{-3} NaCl (aq) at pH 7. A sweep rate of 1 mV s^{-1} was employed in each case.
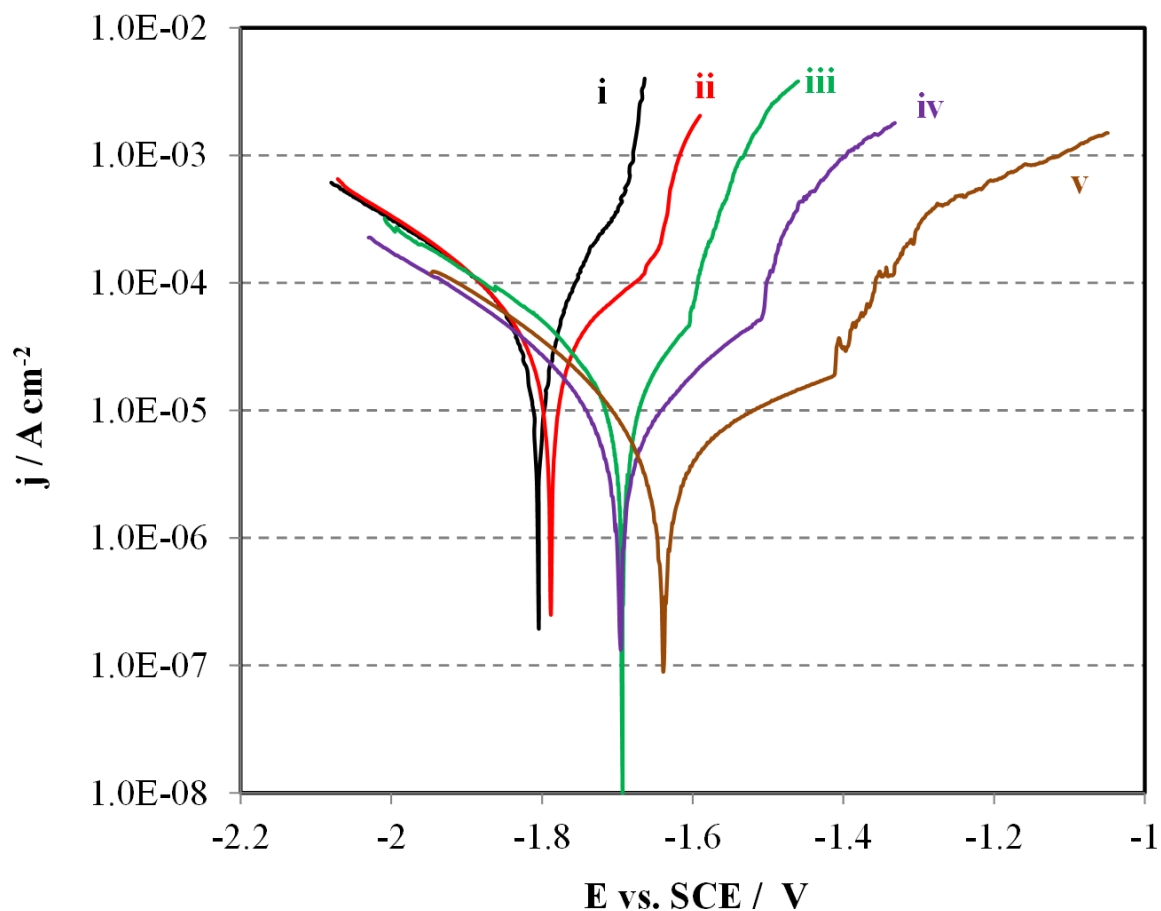
Figure 4: Summary of apparent breakdown potential (E_b) versus chloride ion concentration determined for Mg-As (0.37%) in NaCl-containing electrolyte.
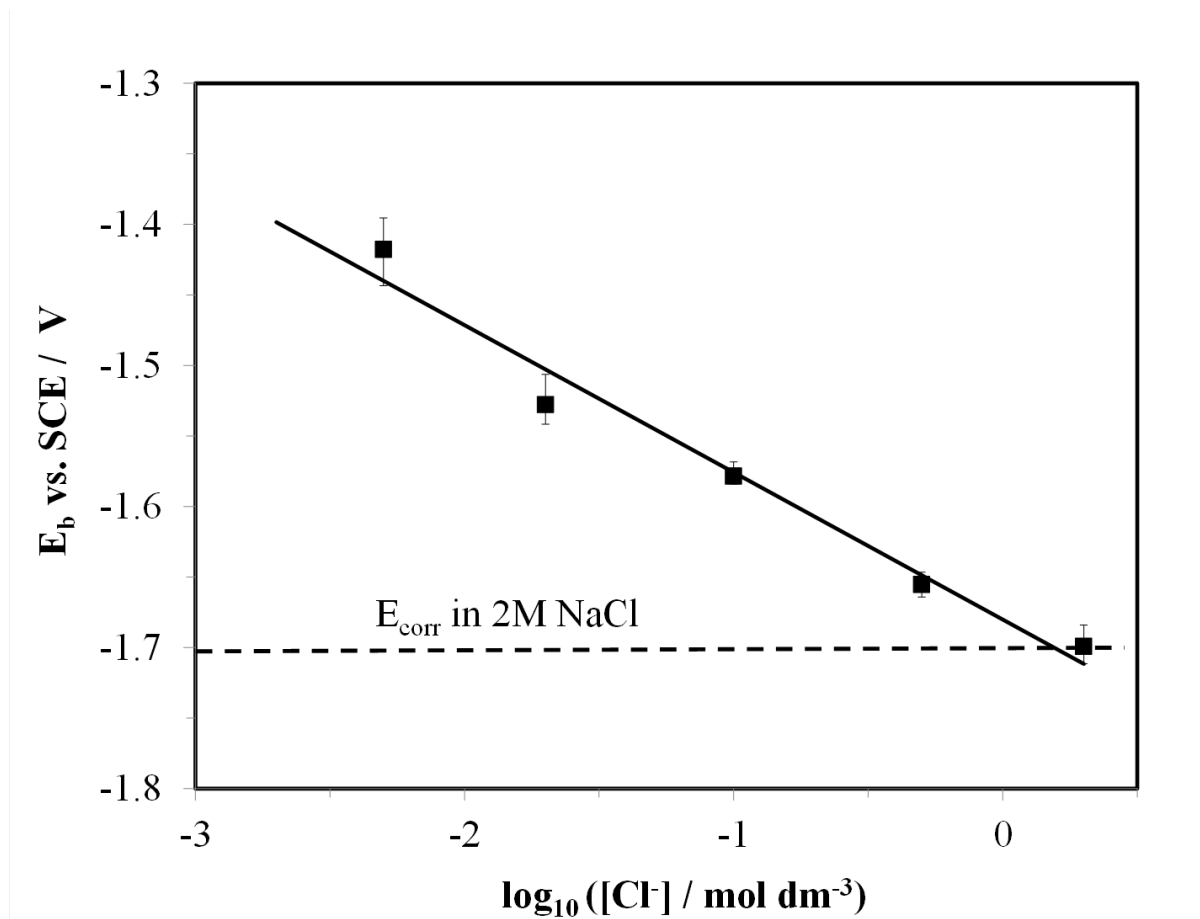
Figure 5: Surface maps of showing j_z distributions associated with a propagating corrosion feature on Mg-As (0.37%) recorded at (a) 15 (b) 16 and (c) 17h following initial immersion in 2 mol dm^{-3} NaCl (aq) at pH 7. (d) shows sample appearance after 24h immersion.
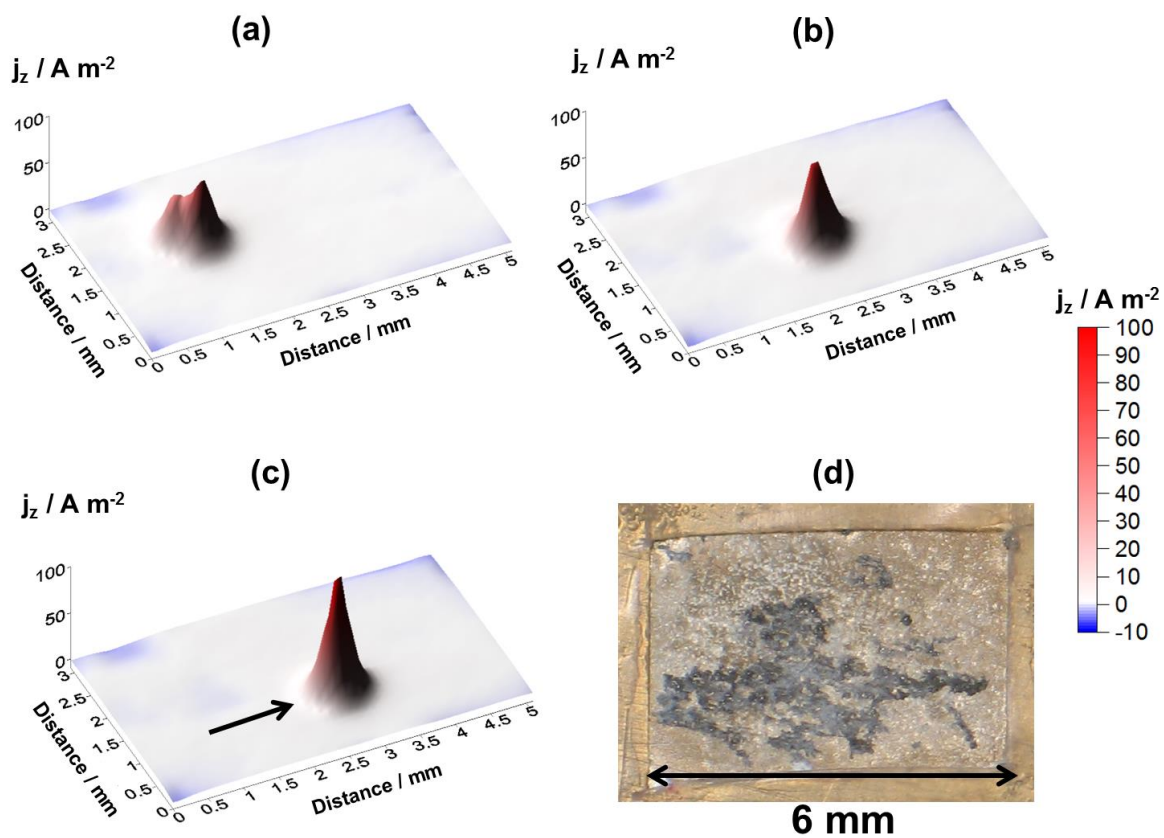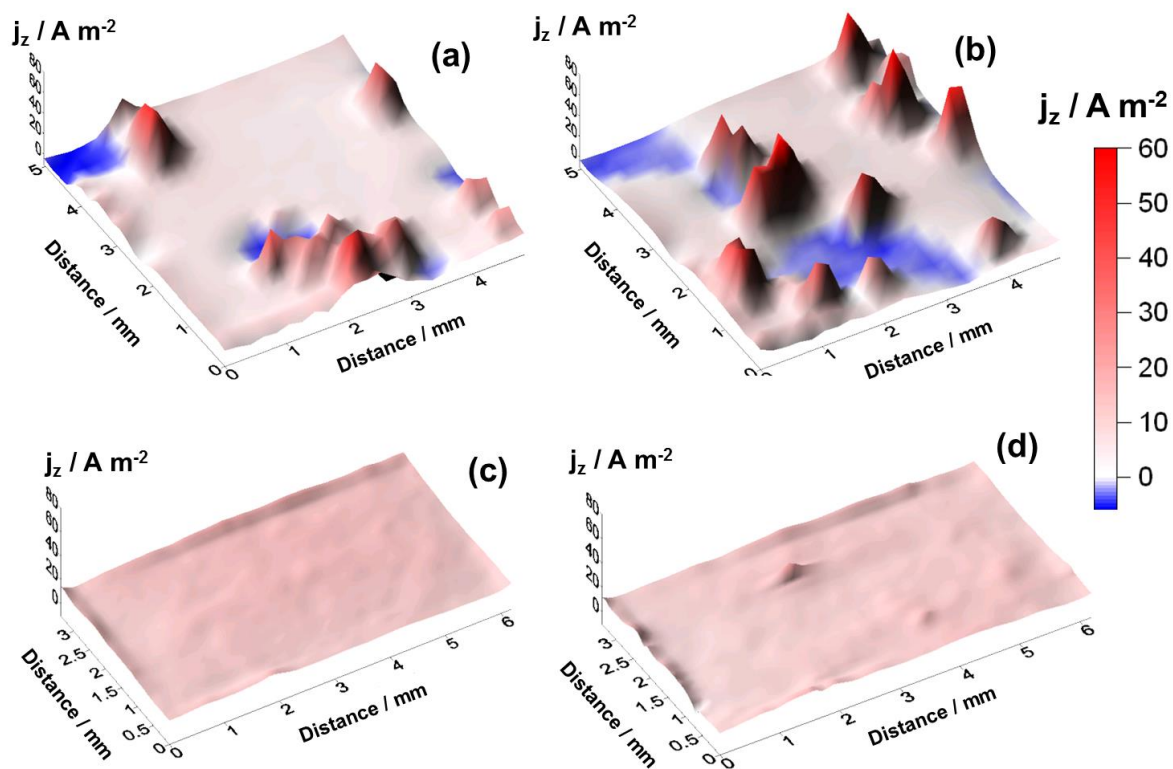
Figure 6: Surface maps of showing j_z distributions associated with propagating corrosion features on pure Mg recorded at (a) 16 (b) 18 and (c) 20h following initial immersion in 2 mol dm^{-3} NaCl (aq) at pH 7. (d) shows sample appearance after 24h immersion.
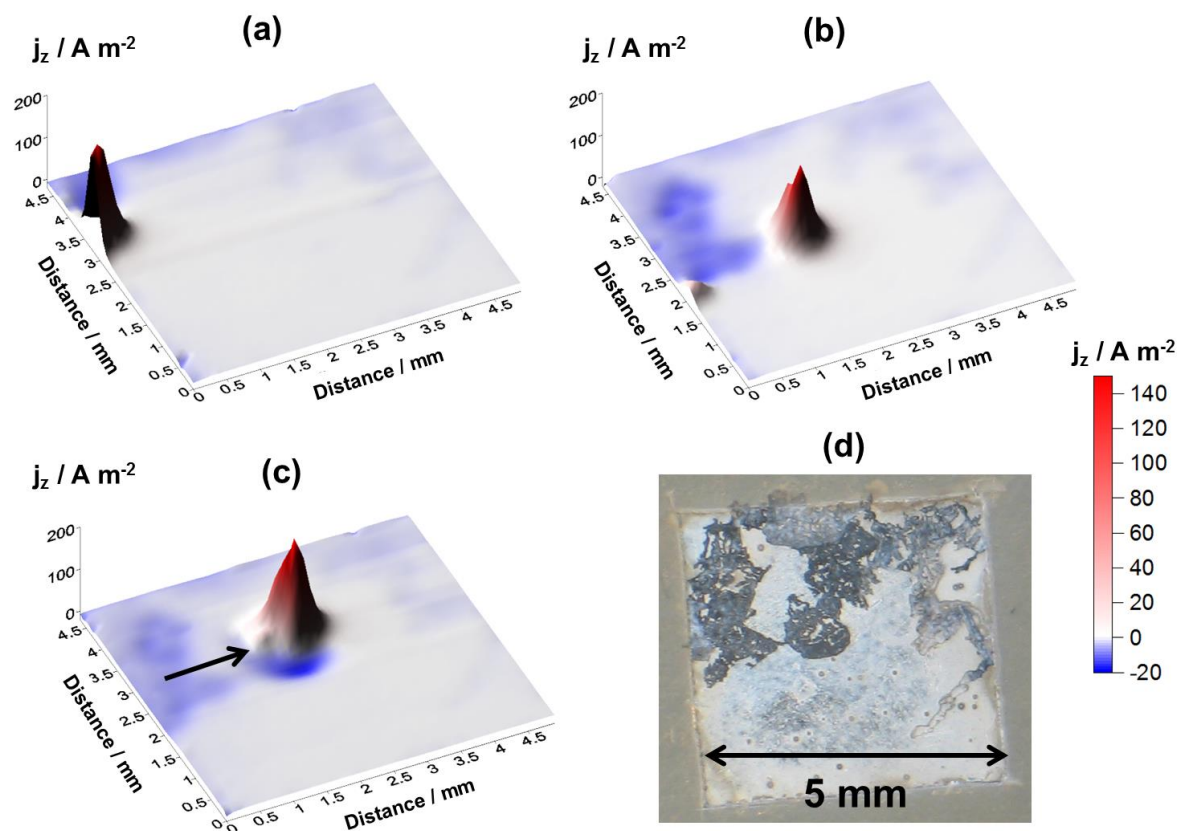
Figure 7: Comparison of local current density (j_z) versus distance profiles for propagating filiform-like corrosion features on Mg observed in 2 mol dm^{-3} NaCl (aq) in the presence (a) and absence (b) of alloyed As (0.37 %).
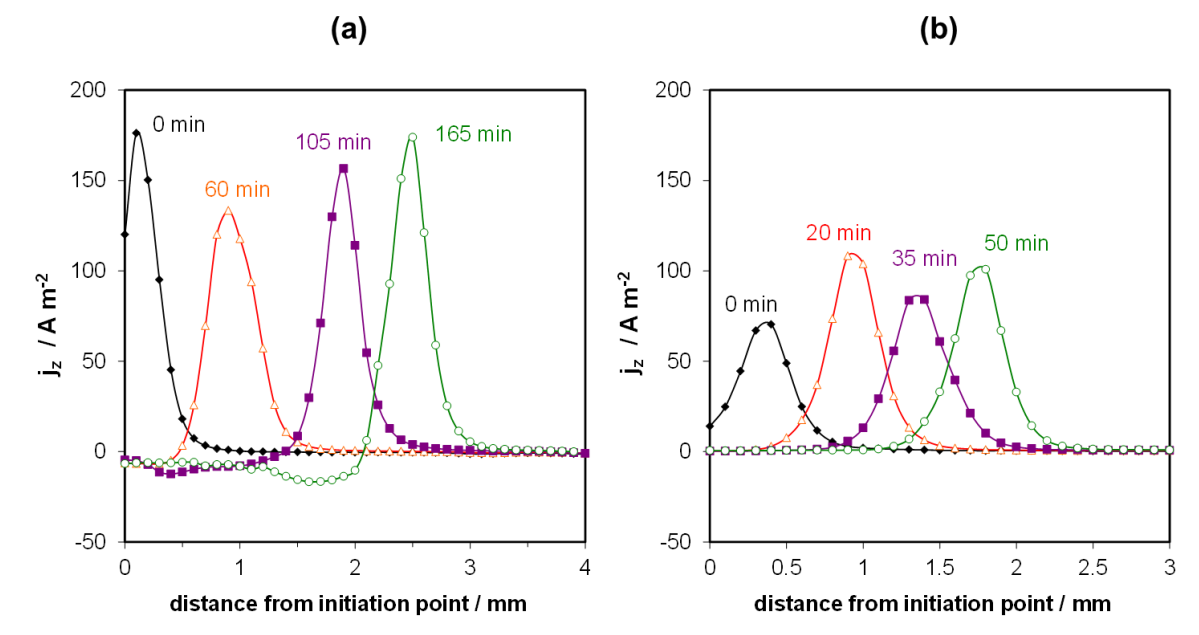
Figure 8: Surface plots showing the distribution of normal current density j_z above both pure Mg (a and b) and Mg-As (0.37%) (c and d) specimens under galvanostatic polarisation using an applied current density +0.4 mA cm^{-2}. Results are shown for specimens held at 60 min (a and c) and 2 h (b and d) in 0.1 mol dm^{-3} NaCl (aq) at pH 7.

Figure 9: Surface plot showing j_z distribution above a Mg-As (0.37%) specimen (a) recorded after 2h of galvanostatic polarisation at 1 mA cm^{-2} in 0.1 mol dm^{-3} NaCl (aq) at pH 7. Images comparing the appearance of pure Mg and Mg-As after 6h anodic polarization are shown in (b) and (c) respectively.
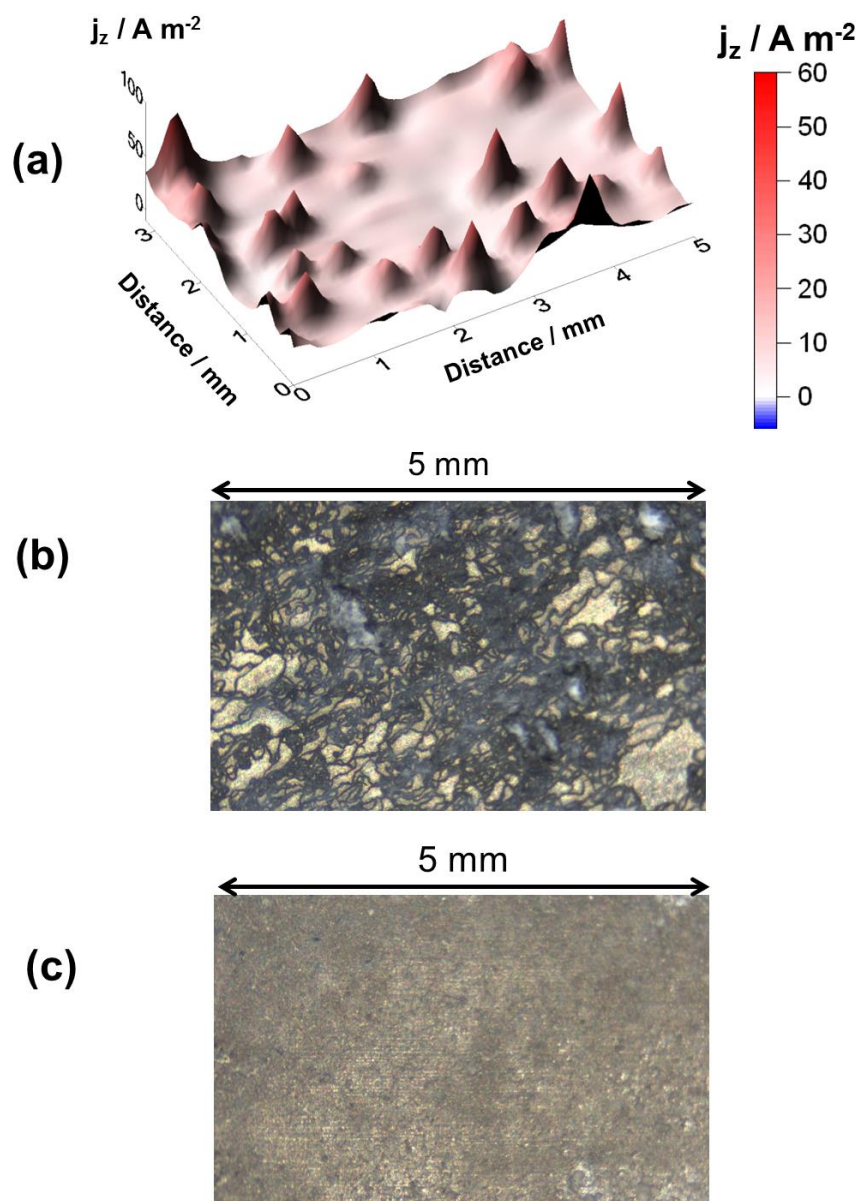
Figure 10: Plots of time dependent SVET-derived integrated current (I_t), normalised for a 1 cm^2 area obtained for pure Mg and Mg-As (0.37%) held under galvanostatic polarisation at +0.4 mA cm^{-2} in 0.1 mol dm^{-3} NaCl (aq).
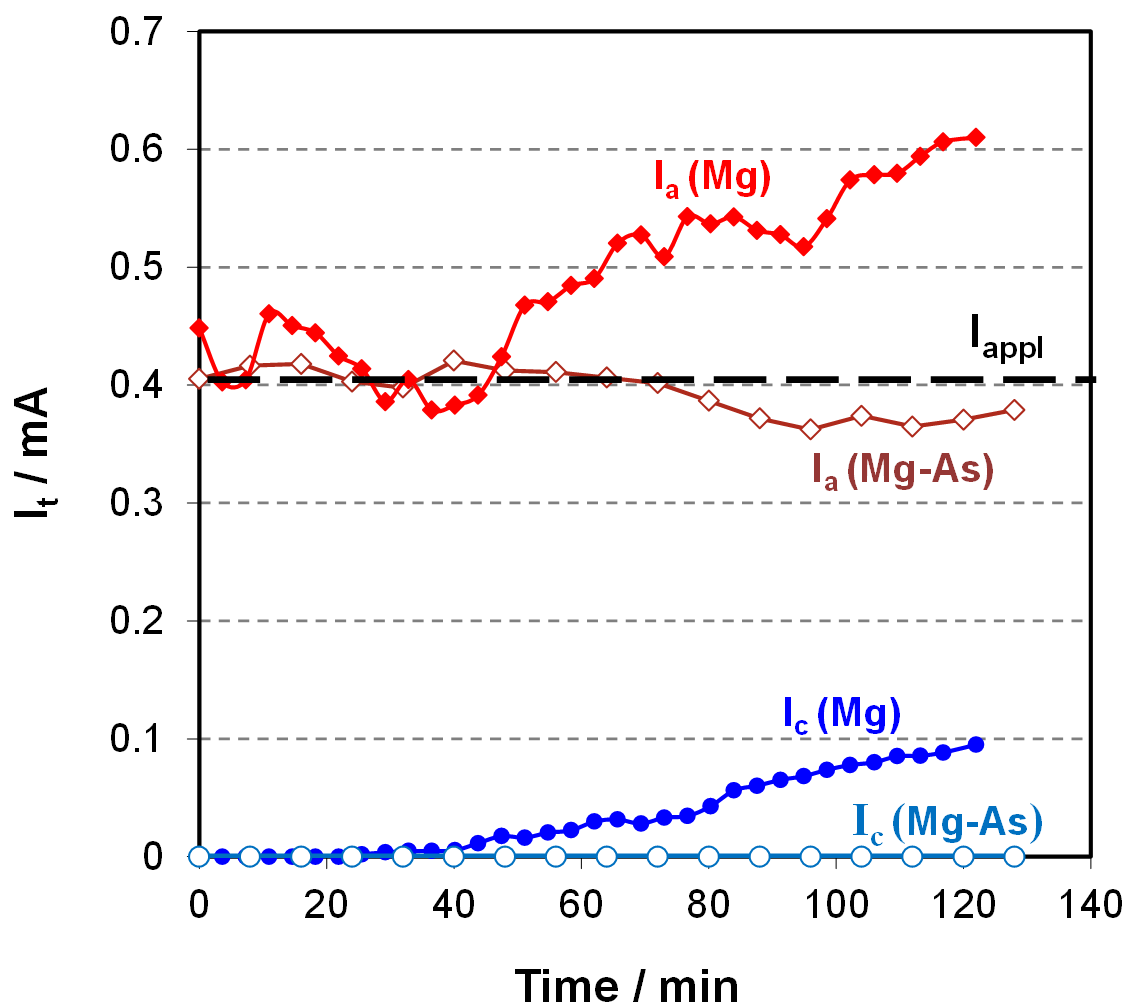
Figure 11: Plots of moles hydrogen gas evolved versus time for Mg and Mg-As (0.37%) under galvanostatic polarisation in 0.1 mol dm^{-3} NaCl at pH 7.